3D Hybrid FEM-BEM Using Whitney Facet Elements and Independent Loops

Douglas Martins Araujo, Gérard Meunier, Olivier Chadebec, Jean Louis Coulomb, Loic Rondot

3-D Hybrid FEM–BEM Using Whitney Facet Elements and Independent Loops

Douglas Martins Araujo[1,2], Gérard Meunier[1], Olivier Chadebec[1], Jean Louis Coulomb[1], and Loic Rondot[2]

[1]Grenoble Electrical Engineering Laboratory, Centre National de la Recherche Scientifique, Université Grenoble Alpes, Grenoble F-38000, France
[2]Research and Development-Power Technology Strategy, Schneider Electric, Grenoble 38100, France

This paper presents a hybrid formulation using Whitney facet elements. This formulation is efficient for the modeling of unbounded 3-D magnetostatic problems. Boundary element method is used to model the unbounded regions and finite element method to model the ferromagnetic ones. Using equivalent circuit representation, the problem is changed, the degrees of freedom becoming magnetic flux in loops instead of faces. As a result, the dimension of the system to be solved is decreased.

Index Terms— Boundary element method (BEM), facet finite elements, hybrid FEM–BEM, magnetostatics.

I. Introduction

NUMERICAL tools based on finite element method (FEM) provide to the user an effective representation of the device. Compared with analytical methods, the geometrical and physical properties are both accurately and quickly described. Furthermore, FEM can solve a wide range of problems. FEM-based models need a full domain representation including magnetic nonlinear regions and the surrounding region. As a result, the number of degrees of freedom (DoFs) can dramatically increase.

To tackle this problem, integral formulations have been considered [1]. Integral volume methods can be used to represent nonlinear regions and consider implicitly the surrounding linear region. A drawback of these methods is the building of a fully populated matrix. Thus, the assembly time can be prohibitive.

The boundary element method (BEM) is used to model linear unbounded regions. In this method, the DoFs are located on the domains interface (bounded and unbounded).

The use of Whitney facet elements for approximation of induction in FEM–BEM magnetostatic formulations has already been proposed in [2]. The originality of our approach is to impose the solenoidality of $\mathbf{b}$ through independent loops techniques associated with an equivalent circuit associated with the dual mesh [3]. This new formulation has been validated thanks to the modeling of a U-shaped contactor and obtained result compared with pure FEM.

II. Magnetostatic Problem

We suppose a magnetic domain $_m$, containing eventually magnets and surrounded by an unbounded domain $_0$ with permeability μ_0. The surrounded region contains a nonmeshed coil in which flows an electric current density $\mathbf{j}$. Fig. 1 shows the problem.

Manuscript received June 8, 2014; revised September 29, 2014; accepted October 17, 2014.

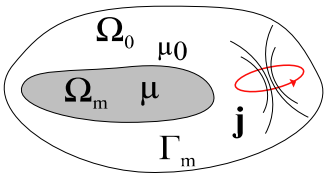

Fig. 1. Classical representation of magnetostatic problem: different domains, materials, and magnetic sources.

To study the distribution of magnetic quantities (as magnetic field $\mathbf{h}$ and induction $\mathbf{b}$) in a given device and neglecting temporal variations, Maxwell's equations for a magnetostatic problem are considered

$$\mathbf{curl}\ \mathbf{h} = \mathbf{j} \tag{1}$$

$$\mathrm{div}\ \mathbf{b} = 0. \tag{2}$$

Magnets may optionally be introduced, leading to the following constitutive Law:

$$\mathbf{b} = \mu(\mathbf{h} - \mathbf{h_c}) \quad \text{where } \mu = \mu(h) \tag{3}$$

where $\mathbf{h_c}$ is the magnet's coercive field.

The total magnetic field is split into two parts, as follows:

$$\mathbf{h} = \mathbf{h}_0 - \mathbf{grad}\ \varphi \tag{4}$$

where φ is the reduced magnetic scalar potential, $\mathbf{h}_0$ is the source field created by the nonmeshed coil, and $\mathbf{h_{red}} = -\mathbf{grad}\ \varphi$ is the reduced magnetic field.

Because $\nu\mathbf{b} = -\mathbf{h_c} + \mathbf{h}$, we have

$$\nu\mathbf{b} = -\mathbf{h_c} + \mathbf{h}_0 - \mathbf{grad}\ \varphi \tag{5}$$

where ν is the magnetic reluctivity.

III. FEM Using Whitney Facet Elements

The total induction $\mathbf{b}$ could be interpolated using facet shape functions, as follows [4]:

$$\mathbf{b}(\mathbf{x}) = \sum_{j}^{N_f} \mathbf{w}_j(\mathrm{x})\ \ _j \tag{6}$$

where $\mathbf{w}_j$ is the j facet shape function, $_j$ is the magnetic flux through the facet j, and N_f is the number of internal and

external faces generated from the discretization. Let us notice the main property of this kind of element family: the normal component of $\mathbf{w}_j$ is conserved through each facet, ensuring the conservation of normal induction. Equation (5) is projected on the domain Ω_m using facet shape functions to get a Galerkin equation

$$\int_{\Omega_m} \mathbf{w}_i \cdot \nu \mathbf{b} d\Omega - \int_{\Omega_m} \mathbf{w}_i \cdot \mathbf{h_{red}} d\Omega = \int_{\Omega_m} \mathbf{w}_i \cdot (-\mathbf{h_c} + \mathbf{h}_0) d\Omega. \quad (7)$$

With (6) and introducing the reduced scalar magnetic potential, we get

$$\sum_j^{N_f} \int_{\Omega_m} \mathbf{w}_i \cdot \nu \mathbf{w}_j \Psi_j d\Omega - \int_{\Omega_m} \mathbf{w}_i \cdot \mathbf{grad}\ \varphi_m d\Omega = \int_{\Omega_m} \mathbf{w}_i \cdot (-\mathbf{h_c} + \mathbf{h_0}) d\Omega. \quad (8)$$

By integrating by parts, the second integral of (8) is

$$\int_{\Omega_m} \mathbf{w}_i \cdot \mathbf{grad}\ \varphi_m d\Omega = \int_{\Gamma_m} \varphi_m \mathbf{w}_i \cdot \mathbf{n} d\Gamma - \int_{\Omega_m} \varphi_m \mathrm{div} \mathbf{w}_i d\Omega. \quad (9)$$

Looking at the right side of (9), both terms could be interpreted as averaged reduced potentials. Because $\mathbf{w}_i \cdot \mathbf{n} = 1/S_i$, S_i being the surface of element i, we can conclude that the first integral represents the averaged potential on this boundary face

$$\int_{\Gamma_m} \varphi_m \mathbf{w}_i \cdot \mathbf{n} d\Gamma = \bar{\varphi}_{\Gamma m}. \quad (10)$$

Similarly, the second integral represents the averaged potential on the volume of elements. Considering an element e and one of its facets j, then $\mathrm{div}\mathbf{w}_j = \pm 1/V_e$, where V_e is the volume of element e, we get

$$\int_{\Omega_m} \varphi_m \mathrm{div} \mathbf{w}_j d\Omega = \Delta\bar{\varphi}_m. \quad (11)$$

Let us notice that the sign of the preceding term depends on the orientation of facet j. Hence, (8) can be rewritten, as follows:

$$[\mathbf{R}]\mathbf{\Psi} - \begin{Bmatrix} \Delta\bar{\varphi}_{\Gamma \mathbf{m}} \\ \Delta\bar{\varphi}_{\mathbf{m}} \end{Bmatrix} = \mathbf{U} \quad (12)$$

where $\Delta\bar{\varphi}_m$ is the variation of averaged potentials between adjacent volumes elements, $\Delta\bar{\varphi}_{\Gamma m}$ is the variation of averaged potentials of a volume element and a face on boundary if the face is located on Γ_m, $\mathbf{\Psi}$ is the magnetic flux through the facets and surface, and $[\mathbf{R}]$ is the stiffness matrix, sparse which is similar to a matrix obtained during a classical FEM assembly, such as

$$R_{ij} = \int_{\Omega_m} \mathbf{w}_i \cdot \nu \mathbf{w}_j d\Omega. \quad (13)$$

$\boldsymbol{U}$ is the source term from coils and magnets, such as

$$U_i = \int_{\Omega_m} \mathbf{w}_i \cdot (-\mathbf{h_c} + \mathbf{h_0}) d\Omega. \quad (14)$$

System (12) can be considered as a matrix representation of an equivalent electric circuit. The centroids of elements of the primal mesh are now the nodes of the dual mesh [5].

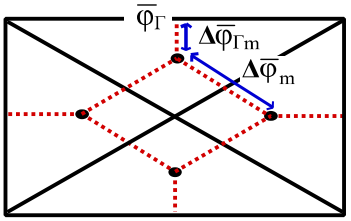

Fig. 2. Primal and dual meshes. Black points: centroid of elements. Dotted lines: branches of the dual mesh. Both of the averaged potential configurations are shown (internal and border branches).

Similarly, the facets of elements of the primal mesh are now the branches of the dual mesh.

Each DoF carries two different quantities. The first one is the magnetic flux of branches and it represents the analogy of electric current for magnetic problems. This flux is the same that crosses the faces and was presented in the previous equations.

This electric circuit has to be completed. To impose $\mathrm{div}\ \mathbf{b} = 0$, a circuit solver will be used (Section V). Fig. 2 shows an example of dual mesh used to build an equivalent circuit from the primal mesh and the different potential averages involved.

The external part of the circuit has to be considered. BEM involves two quantities: the magnetic potential and the magnetic flux on boundary. This will allow us to develop a perfect coupling between the method presented above and the BEM and complete the electric circuit.

IV. Boundary Element Method

The main idea is to solve Laplace equation transforming the volume integral equation over all domain Ω_0, into a surface integral on the boundary Γ_m. This transformation can be made thanks to Green's identity [6].

Considering the third Green's identity applied in the air region to the reduced magnetic potential φ, we get

$$c(\mathbf{x_0})\varphi(\mathbf{x_0}) = \int_{\Gamma_m} \left(\nabla_n G(\mathbf{x_0}, \mathbf{x}) \varphi - G(\mathbf{x_0}, \mathbf{x}) \left(\frac{1}{\mu_0} \mathbf{b} - \mathbf{h_0} \right) \cdot \mathbf{n} \right) d\Gamma \quad (15)$$

where $\varphi(\mathbf{x_0})$ is the reduced magnetic scalar potential at $\mathbf{x_0}$ point, $G(\mathbf{x_0}, \mathbf{x})$ is the 3-D Green's function $(1/r)$, r is the norm of a distance vector linking $\mathbf{x_0}$ and a point $\mathbf{x}$ of the boundary, and $c(\mathbf{x_0})$ is the solid angle subtended by the boundary Γ_m at $\mathbf{x_0}$.

Let us consider a uniform distribution for the potential and its normal derivative on the border (zero-order interpolation function for both equivalent to degenerated facet shape functions on Γ_m) [4]

$$\varphi(\mathbf{x}) = \sum_j^{N_\Gamma} w_j(\mathbf{x}) \varphi_j, \quad \Psi(\mathbf{x}) = \sum_j^{N_\Gamma} w_j(\mathbf{x}) \frac{\Psi_j}{S_j} \quad (16)$$

where $\Psi_j = b_{nj} S_j$ and N_Γ is the number of facets of the boundary. By applying Galerkin projection to (15) and choosing the same weighting functions and interpolation functions used to describe reduced magnetic potential and normal

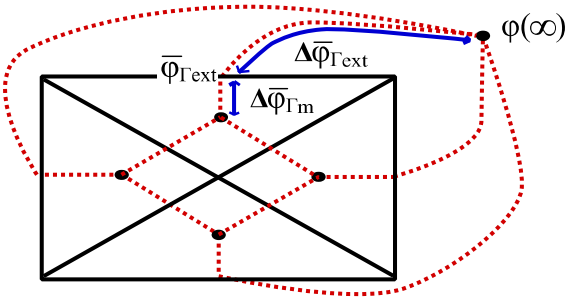

Fig. 3. Primal and dual meshes. Black points: centroid of elements and the imposed potential at the infinite. Internal and external contributions are represented.

magnetic induction distributions (16), we get

$$[\mathbf{H}]\varphi_{\Gamma ext} + [\mathbf{T}]\Psi_{\Gamma} = [\mathbf{T_1}]\mathbf{h_{0n}}. \tag{17}$$

$[\mathbf{T}]$, $[\mathbf{T_1}]$, and $[\mathbf{H}]$ matrices are associated to the following expressions:

$$T_{ij} = \int_{\Gamma_{mi}} \frac{1}{\mu_0 S_j} \int_{\Gamma_{mj}} G(\mathbf{x}_i, \mathbf{x}_j) d\Gamma d\Gamma, \quad T_{1ij} = S_j T_{ij}$$
$$H_{ij} = \int_{\Gamma_{mi}} \left(c_{ii} - \int_{\Gamma_{mj}} \nabla_n G(\mathbf{x}_i, \mathbf{x}_j) d\Gamma \right) d\Gamma \tag{18}$$

where c_{ii} is similar to 2π, integration point being located on the regular Γ_m surface. There are many ways to perform integration of (18) [7]. The simple layer potential integral is computed thanks to well-known analytical expression. Integral associated with double layer is expressed thanks to a Gaussian quadrature rule. Let us notice that $[\mathbf{H}]$ matrix is an invertible one.

V. Coupling Both Methods

As Fig. 3 shows, the circuit built using the dual mesh will be completed by adding the contribution of the external reduced potential averaged in the air $\Delta\bar{\varphi}_{\Gamma ext}$. BEM will be used to evaluate this potential.

Because the potential is imposed $\varphi(\infty) = 0$, we get

$$\Delta\bar{\varphi}_{\Gamma ext} = \varphi_{\Gamma} - \varphi(\infty). \tag{19}$$

To ensure the solenoidality of $\mathbf{b}$, a variational formulation can be used [2]. In our approach, a circuit solver resolution based on the determination of independent loops [8] is used. The general principle consists in finding small topological loops, by minimizing the number of branches, allowing a very quick research of independent loops.

The boundary condition can be easily considered in the formulation, by simply suppressing the associated DoFs in the equivalent circuit located on Γ_m. There are no nodes of the dual mesh at the magnetic boundary and the last branch connects the centroid of a volume element and the infinite node

$$\mathbf{\Delta\bar{\varphi}_{\Gamma}} = \mathbf{\Delta\bar{\varphi}_{\Gamma m}} + \mathbf{\Delta\bar{\varphi}_{\Gamma ext}}. \tag{20}$$

The last term of (20) is deduced from (17), as follows:

$$\mathbf{\Delta\bar{\varphi}_{\Gamma ext}} = [\mathbf{H}]^{-1}[\mathbf{T_1}]\mathbf{h_{0n}} - [\mathbf{H}]^{-1}[\mathbf{T}]\Psi_{\Gamma}. \tag{21}$$

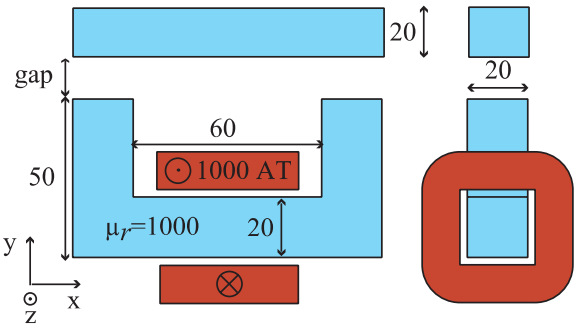

Fig. 4. Magnetic circuit with a linear permeability and a nonmeshed coil.

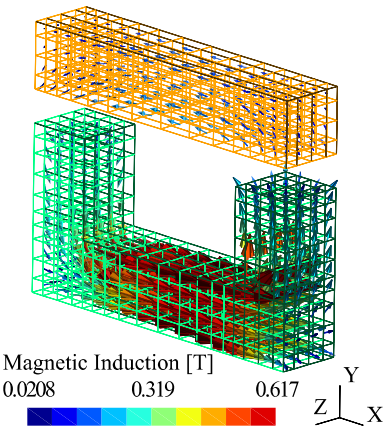

Fig. 5. Distribution of magnetic induction.

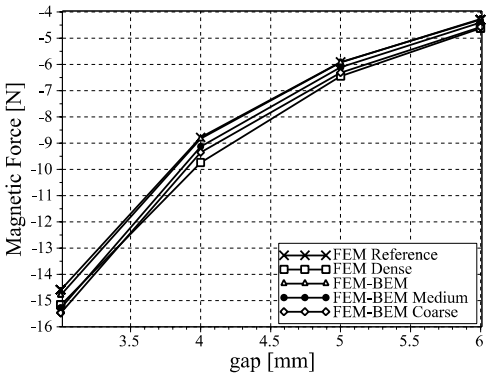

Fig. 6. Comparison between FEM and the formulation presented for the computation of magnetic force.

Fundamental circuit equations are expressed in terms of external and internal average potentials

$$[\mathbf{M}] \begin{Bmatrix} \mathbf{\Delta\bar{\varphi}_{\Gamma}} \\ \mathbf{\Delta\bar{\varphi}_{m}} \end{Bmatrix} = \mathbf{0} \tag{22}$$

where $[\mathbf{M}]$ is the branch-loop matrix. By correlating (12), (21), and (22), we get

$$[\mathbf{M}]\left[\mathbf{R} + \begin{bmatrix} [\mathbf{H^{-1}T}] & 0 \\ 0 & 0 \end{bmatrix}\right][\mathbf{M}]^{\mathbf{t}}\mathbf{\Psi_M} = [\mathbf{M}]\left[\mathbf{U} + \begin{bmatrix} [\mathbf{H^{-1}T_1}]\,\mathbf{h_{0n}} \\ 0 \end{bmatrix}\right] \tag{23}$$

where $\mathbf{\Psi_M}$ is the loop's magnetic flux. By solving the linear system, we obtain the currents flowing on each branch by applying the following equation: $\mathbf{\Psi} = [\mathbf{M}]^{\mathbf{t}}\mathbf{\Psi_M}$.

TABLE I
DEGREES OF FREEDOM

METHOD	FEM 2nd Reference	FEM dense	FEM-BEM	FEM-BEM Medium	FEM-BEM Coarse
DOF	198,207	4,700	1,792	1,216	148

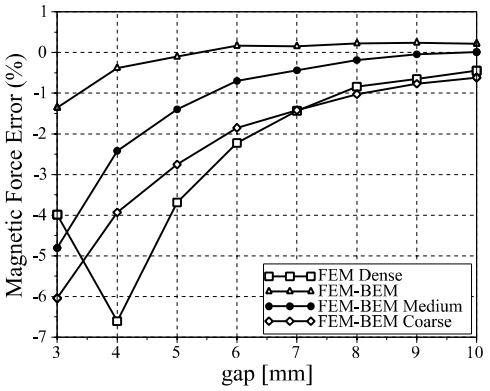

Fig. 7. Relative error for magnetic force. FEM with very dense mesh is the reference.

VI. RESULTS

Fig. 4 shows a magnetic circuit with a coil. The distribution of magnetic induction was studied and it is shown in Fig. 5.

The magnetic force versus variation of the air gap is considered and compared with an FEM reference (Fig. 6) computed with a very dense mesh. Meshes with different number of DoFs are considered: FEM reference, FEM dense, FEM–BEM, FEM–BEM medium, and FEM–BEM coarse (Table I).

Once the problem has been solved, the numerical evaluation of magnetic force is achieved thanks to sources method [9].

Fig. 7 shows the relative error of each solution, FEM with a very dense mesh being used as reference. The new B-oriented H(div)-conforming formulation provides increased accuracy on the normal component of the magnetic induction. Therefore, it is well adapted to magnetic forces evaluations in which good accuracy is obtained using only a very few DoFs. This is the main advantage of our approach compared with the classical FEM–BEM formulation [10].

This comparison was used to validate our new approach. The convergence analysis shows that for the real case FEM–BEM is outperforming FEM in terms of DoF for the magnetic force evaluation. Further discussions concerning computation time, when accelerating techniques are applied, have been extensively made in [11].

VII. CONCLUSION

In this paper, we have presented an original hybrid FEM–BEM formulation using facet elements. The formulation has a small relative error in comparison with a 3-D reference FEM with a high mesh density. The convergence of the results is quickly reached and with very coarse meshes, we get acceptable results. This new formulation seems very attractive because it enables an easy treatment of the unbounded region without meshing the air. Coupling of FEM and BEM by using Whitney facet elements which degenerate to zero-order shape function on the boundary is natural and does not necessitate interpolation process. Moreover, multiple connected regions are naturally treated.

The obtained matrix is composed of a fully dense matrix from BEM and sparse matrix from FEM. Using equivalent circuit representation, the problem is changed, the DoF becoming magnetic flux in loops instead of faces. As a result, the dimension of the system to be solved is decreased.

As we have no element in the unbounded region, the total number of DoF decreases drastically. If the number of elements on the boundary increases, the time spent on the matrix integration and solving becomes prohibitive. However, to solve problems involving a high number of DoF, numerical techniques can be used to reduce time and memory storage consumption. Using, for example, fast multipole acceleration technique, we observe a great reduction in computation time [11].

REFERENCES

[1] A. Carpentier, N. Galopin, O. Chadebec, and G. Meunier, "Modeling of magneto-mechanical coupling using magnetic volume integral and mechanical finite-element methods," *IEEE Trans. Magn.*, vol. 50, no. 2, pp. 233–236, Feb. 2014, Art. ID 7005604.

[2] B. Bandelier and F. Rioux-Damidau, "A mixed B-oriented FEM for magnetostatics in unbounded domains," *IEEE Trans. Magn.*, vol. 38, no. 2, pp. 373–376, Mar. 2002.

[3] A. M. Vishnevsky, A. G. Kalimov, and A. A. Lapovok, "Modeling magnetization using Whitney facet elements," *IEEE Trans. Magn.*, vol. 38, no. 2, pp. 489–492, Mar. 2002.

[4] P. Dular, J.-Y. Hody, A. Nicolet, A. Genon, and W. Legros, "Mixed finite elements associated with a collection of tetrahedra, hexahedra and prisms," *IEEE Trans. Magn.*, vol. 30, no. 5, pp. 2980–2983, Sep. 1994.

[5] A. Bossavit, "Mixed-hybrid methods in magnetostatics: Complementarity in one stroke," *IEEE Trans. Magn.*, vol. 39, no. 3, pp. 1099–1102, May 2003.

[6] F. Boeykens, H. Rogier, J. Van Hese, J. Sercu, and T. Boonen, "Efficient calculation of coupling matrices for a decoupled FE/BIE formulation," in *Proc. ICEAA*, Sep. 2012, pp. 506–509.

[7] A. Aimi and M. Diligenti, "Hypersingular kernel integration in 3D Galerkin boundary element method," *J. Comput. Appl. Math.*, vol. 138, no. 1, pp. 51–72, Jan. 2002.

[8] T.-S. Nguyen, J.-M. Guichon, O. Chadebec, G. Meunier, and B. Vincent, "An independent loops search algorithm for solving inductive PEEC large problems," *Prog. Electromagn. Res. M*, vol. 23, pp. 53–63, 2012.

[9] S. Bobbio, F. Delfino, P. Girdinio, and P. Molfino, "Equivalent sources methods for the numerical evaluation of magnetic force with extension to nonlinear materials," *IEEE Trans. Magn.*, vol. 36, no. 4, pp. 663–666, Jul. 2000.

[10] G. Meunier, J.-L. Coulomb, S. Salon, and L. Krähenbühl, "Hybrid finite element boundary element solutions for three dimensional scalar potential problems," *IEEE Trans. Magn.*, vol. 22, no. 5, pp. 1040–1042, Jan. 1986.

[11] R. V. Sabariego, J. Gyselinck, P. Dular, C. Geuzaine, and W. Legros, "Fast multipole acceleration of the hybrid finite-element/boundary-element analysis of 3-D eddy-current problems," *IEEE Trans. Magn.*, vol. 40, no. 2, pp. 1278–1281, Mar. 2004.